This is a previous version of the article published in Materials Research Bulletin. 2021, 134: 111089. https://doi.org/10.1016/j.materresbull.2020.111089

Study of MWCNT Dispersion Effect in TiO_2-MWCNT Composites for Gas-Phase Propene Photooxidation

J. Fernández-Catalá, Á. Berenguer-Murcia and D. Cazorla-Amorós *

Materials Institute and Inorganic Chemistry Department, University of Alicante, Ap. 99, E-03080 Alicante, Spain.

**Corresponding author; e-mail: cazorla@ua.es*

Abstract

In this study, we have performed the synthesis of TiO_2-MWCNT composites focusing on the distribution of the photoactive phase on the carbon active sites existing in the MWCNTs, and its effect on the properties of the composites for the abatement of propene. We have used different approaches for the dispersion of MWCNTs during the synthesis; 1) an ultrasound bath for 5 minutes, 2) an ultrasound bath for 60 minutes, and 3) an ultrasound probe for 5 min. We observed that the incorporation of MWCNTs in the TiO_2 synthesis improves the catalytic activity in the photooxidation of propene, but the best results are obtained for ultrasound probe treatment. A good dispersion of the MWCNT and an increase in the active surface area or surface oxygen functionalities of the MWCNTs are key factors to achieve an improved photocatalytic activity for total propene oxidation, thus benefitting from the synergy between TiO_2 and MWCNT.

Keywords: A. TiO_2, A. MWCNT, A. Composites, B. Sol-gel synthesis, D. Photocatalytic activity.

Graphical abstract

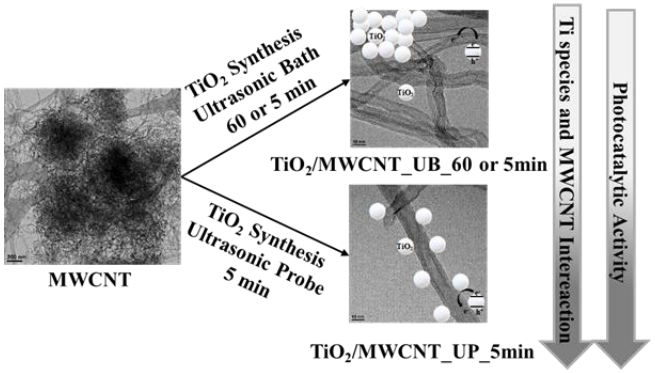

Research highlights

- A facile preparation method of MWCNT and TiO_2 composites is presented.
- The presence of MWCNT improved the photocatalytic activity of the TiO_2.
- The use of an ultra sound probe in the MWCNT dispersion increases the ASA of MWCNT.
- A better interaction of TiO_2 and MWCNT improves the photooxidation of propene.

1. Introduction

Titanium dioxide (TiO_2) has attracted a great interest in recent decades for photocatalytic reactions such as water splitting, CO_2 reduction, and VOCs abatement, among others [1-4]. This is due to its attractive properties such as chemical stability, low cost and resistance to corrosion. However, this material presents some limitations, for example large band gap, high electron-hole (e^- h^+) recombination rate and low surface area that limit its catalytic activity [3,5,6]. For these reasons, the scientific community has performed numerous studies in order to improve these limitations, such as synthesis of nano-TiO_2, TiO_2 doping by incorporation of metals or/and non-metals, and synthesis of TiO_2 composites, among others [3,7-10].

The incorporation of carbon materials (carbon nanotubes, activated carbon, or graphene) on TiO_2 is gaining interest in the photocatalysis field [11-12]. Specifically, the use of carbon nanotubes (CNT) has attracted a significant interest for their use in composite materials (TiO_2-CNT) in photocatalysis applications due to their interesting properties. In this case, the incorporation of CNTs in the photocatalytic system enhances the lifetime of generated electron-hole (e^--h^+) pairs in the TiO_2 and they can provide supplementary catalytic active sites under certain reaction conditions, among other properties [11-15].

In this sense, Vincent et al reported the incorporation of carbon nanotubes (CNTs) with a TiO_2 prepared by a sol-gel method indicating different applications of this type of nanocomposite [16]. Yu et al observed that the presence of CNTs in the TiO_2 can change the properties of TiO_2. In this sense, they observed that the presence of CNTs can modulate the agglomeration of the particles as well as the particle size of the TiO_2 in the composites. In this study it was also observed that the CNTs can suppress the recombination of photo-generated e^--h^+ pairs. However, one drawback is that an excessive

incorporation of CNTs shields the TiO_2 from the absorption of UV light. Concerning the photocatalytic activity of these samples, the composites present an improved photocatalytic activity with respect to P25 and TiO_2-activated carbon (AC) composites in the degradation of acetone [17]. Wang et al observed a synergetic effect in the composite catalysts (TiO_2-MWCNT) improving the photocatalytic activities for conversion of phenol in aqueous solutions [18]. Koli et al investigated the photocatalytic activity of the degradation of methyl orange dye and the photo-inactivation of Bacillus subtilis, using TiO_2-MWCNT composites. In both applications, the authors observed a significant enhancement in the degradation/inactivation reaction rate with the TiO_2-MWCNTs (0.5 wt.%) with respect to bare TiO_2 [19].

With this in mind, this study focuses on the preparation of TiO_2-MWCNT composites through the incorporation of dispersed and active MWCNT **by different sonication methodologies** in the TiO_2 synthesis solution in order to improve the photocatalytic activity of the pure TiO_2 material **through an improved TiO_2-Carbon interaction. In this respect the activation of CNTs for preparation of these composites is generally carried out using HNO_3 which can drastically modify the properties of the carbon material [20]. For this reason, we have done an exhaustive study of the effect of the distribution of the photoactive phase and presence of active sites in the MWCNT using sonication in the properties of the final composite in terms of their catalytic properties, focusing in the characterization and with the aim of understanding the effect of active sites in the MWCNT in the synthesis of composites since this has not been fully explored to date.**

With the objective of testing the catalytic activity of these composites in an application of current interest, the samples have been tested in the abatement of propene at low concentrations since this contaminant is considered a model for low molecular weight

Volatile Organic Compounds (VOCs) [21-23]. From this study, we understand the experimental conditions and the properties of the MWCNT that permit the synthesis of an optimized TiO_2-MWCNT powdered material for the photocatalytic oxidation of propene.

2. Experimental section

2.1 Materials

Titanium (IV) tetrabutoxide (TTB, 97%, Sigma-Aldrich), absolute ethanol (EtOH, 99.8%, Fisher Scientific), Multiwall Carbon Nanotubes (MWCNT, Columbian Chemical Company), urea (99%, Merck), Pluronic F-127 (F-127, Sigma-Aldrich), formamide (FA, 99.5%, Sigma-Aldrich), glacial acetic acid (HAc, 99%, Sigma-Aldrich), and deionized water were used as received in this study.

2.2 Preparation

TiO_2-MWCNT composites were prepared through the modification of a previously published synthesis of TiO_2, developed in our research group [24]. The main difference was the incorporation of the required amount of a suspension of commercial MWCNTs in the synthesis medium of TiO_2 to yield a 1 wt. % loading of MWCNT. **Higher CNTs loadings were found to shield the TiO_2 from absorbing UV light causing a significant drop in the catalytic activity of TiO_2 under UV radiation [17].**

The TiO_2-MWCNT composites synthesis was performed as follows: 5 g of titanium tetrabutoxide (TTB) were weighed and dissolved in 7.9 g of absolute EtOH. This solution (labelled “solution A”) was stirred for 10 min. Then, 1.6 g of deionized water, 7.9 g of EtOH, 0.3 g of F-127, 0.4 g of FA, 0.4 g of urea, and 1.6 g of HAc were weighed and added in a separate vessel and the mixture was stirred for 10 min (labelled “solution B”). Then, the MWCNTs were added to solution B and then dispersed following three

different approaches. In the first and second approach the MWCNTs were dispersed for 5 min and 60 min using an ultrasonic bath (Fisherbrand, FB15051) with a power of 200 W and in the third approach the MWCNTs were dispersed with an ultrasound probe (Bandelin SONOPULS HD 2200) for 5 min with a power of 660 W operating at 30% output power. Once, the MWCNTs had been dispersed, "Solution B" was added dropwise on "solution A" under stirring. The resulting solution was transferred to a 40 mL autoclave and heated at 60 °C for 24 h. The temperature was later increased to 120 °C for another 24 h. The samples obtained were calcined at 350 ºC for 6 h with a heating rate of 1 °C/min. The nomenclature used for the samples were TiO_2-MWCNT_UB_5min and TiO_2-MWCNT_UB_60min for the samples where the MWCNTs were dispersed for 5 min and 60 minutes using an ultrasonic bath, respectively, and TiO_2-MWCNT_UP_5min for the samples where the MWCNTs were dispersed for 5 min with an ultrasound probe. Moreover, in this study a commercial P25 (TiO_2) sample and a sample of pure TiO_2, prepared without addition of MWCNT suspension, were used for comparison purposes.

2.3 Samples Characterization

The amount of MWCNTs in the composites (TiO_2-MWCNT) was obtained from the weight loss in the 450-600 ºC interval measured by thermogravimetric analysis (TG analysis) using a thermobalance (SDT 2960). The sample was heated up to 900 °C in air, using a heating rate of 5 °C min^{-1} in the aforementioned equipment.

The TiO_2 crystallinity and crystal phase composition were determined by X-ray diffraction (XRD) analysis using a Miniflex II Rigaku apparatus using Cu Kα radiation and a scanning rate of 2º/min, in the 2θ range 6-80°.

The optical absorption properties of the materials were studied by UV-VIS/DR spectroscopy (Jasco V-670). $BaSO_4$ was used as the reference standard. The band gap energy was calculated by the absorbance method [25] as follows (Equation 1):

$$Eg=\frac{1239.8}{\lambda} \quad (1)$$

where Eg is the band gap energy (eV) and λ is the edge wavelength (nm).

The morphology analysis of the materials was performed by transmission electron microscopy (TEM, JEOL JEM 2010) and Field-emission scanning electron microscopy (FE-SEM, ZEISS, Merlin VP Compact).

The ASA (Active Surface Area) of the MWCNT samples prepared in this work was measured using an established method which is based on di-oxygen chemisorption [26,27]. Firstly, 10 mg of MWCNT (only carbon material) were heat-treated up to 920 ºC at a heating rate of 20 ºC/min under a N_2 flow rate of 100 mL/min, and kept at 920 ºC for 0.5 h under N_2 to remove all oxygen functional groups from the carbon surface. Then, the temperature is lowered to 250 ºC and kept for 1 h under inert atmosphere. Then, synthetic dry air (20 vol% O_2 in N_2) is fed to the thermobalance for 7 h to perform the oxygen chemisorption step. The ASA was estimated from the weight uptake of the samples by the following equation (Equation 2) assuming that each chemisorbed oxygen atom occupies an area of 0.083 nm^2:

$$ASA\ (m^2/g)=\frac{1}{w_0}\cdot\frac{A\cdot N_A\cdot(w_c-w_0)}{N_O} \quad (2)$$

where A is the area that one oxygen atom occupies per edge site (carbon atom), N_A is the Avogadro constant, w_0 is the starting weight of carbon in the chemisorption step, w_c is the weight of carbon after oxygen chemisorption and N_O is oxygen atomic weight.

The characterization of the surface functionalities of carbon materials was analyzed by Temperature-Programmed Desorption (TPD) measurements [28,29]. TPD experiments were performed in a thermogravimetric system (TA Instruments, SDT Q600 Simultaneous) coupled to a mass spectrometer (Thermostar, Balzers, BSC 200). In order to obtain the TPD analysis, the MWCNTs were heat-treated up to 920 ºC at a rate of 20

ºC/min followed by a dwelling time of 0.5 h under a Helium flow rate of 100 mL/min. The CO and CO_2 evolved from the samples during the heat treatment was monitored by mass spectrometry. The amounts of CO and CO_2 desorbed from the samples during the experiments were quantified by calibration of 28 and 44 $m \cdot z^{-1}$ signals using calcium oxalate.

2.4 Catalytic Tests

The photocatalytic performance in propene photooxidation at low concentration of the different composites prepared in this work was studied in an experimental set up previously reported in our research group [24,30]. This experimental set-up is based on a vertical quartz reactor (50 mm in height and 20 mm in diameter) where the photocatalyst was placed on a quartz wool bed (10 mm in height). A commercial UV lamp with the radiation peak at 365 nm (Philips, TL 8W/05 FAM, 1W,) irradiated the quartz reactor, along with the photocatalyst, in a parallel position at a distance of 1 cm. The UV lamp and quartz reactor with the photocatalyst was surrounded by a cylinder covered with aluminum foil.

The materials synthesized in this work were tested in the photomineralization of propene at low concentration (100 ppmv in air) at room temperature (calibrated gas cylinder was supplied by Carburos Metálicos, S.A.) under flow conditions. The tests were carried out using a flow of a propene-containing stream of 30 (STP) ml/min. Firstly, the photocatalyst (0.11g) was incorporated in the quartz reactor and then the reactor was purged with helium to clean the surface of the catalyst. The propene-containing stream was passed through the photocatalyst bed until propene concentration reached a stable reading (after about 3 h). In this moment the lamp was switched on and kept working until steady state conditions were reached (usually after 3 h) and, during the experiment, the outlet gas was continuously analyzed by mass spectrometry (Balzers, Thermostar GSD 301 01).

Propene conversion was estimated using the following equation (Equation 3):

$$\text{Propene conversion } (\%) = \frac{C_{initial_{C_3H_6}} - C_{steady\ state_{C_3H_6}}}{C_{initial_{C_3H_6}}} \times 100 \quad (3)$$

where $C_{initial\ C3H6}$ is the initial propene concentration, 100 ppmv and $C_{steady\ stateC3H6}$ is the propene concentration at steady state conditions (usually after 3 h) in the outlet gas when the UV light is switched on. **The catalytic reactions were performed by triplicate and the error obtained in the aforementioned experimental set-up was 2 % in the catalytic measures. The error bars have been included in the photocatalytic activity plots.**

3. Results and Discussion

3.1 Materials Characterization

The carbon loadings (MWCNTs) incorporated in the synthesized composites are collected in Table 1. These results obtained by TG analysis show that all composites present approximately 1 wt% of carbon using the different dispersion approaches. Moreover, these values are similar to the nominal loading value (1 wt.%) indicating that MWCNTs are adequately incorporated in the composites in all approaches studied in this work.

Table 1. Loadings of multiwall carbon nanotubes (MWCNTs) in the composites calculated by TG analysis (determined from the weight loss in the interval 450-600 ºC).

Samples	wt.% MWCNT TG analysis
TiO_2-MWCNT_UB_5min	1.03
TiO_2-MWCNT_UB_60min	0.98
TiO_2-MWCNT_UP_5min	1.06
TiO_2	-

The XRD patterns of the composites prepared using different approaches in the synthesis are showed in Figure 1. In all composites, the TiO_2 presents the characteristic peaks of the anatase phase and they are similar to the bare TiO_2 [24]. **However, the (002) and (100) peaks of MWCNT observable at 26 º and 46 º were not discernable in the composites given the low amount of carbon material present in the composites together with the fact that the characteristic peak of anatase TiO_2 appears at 25.3 º overlapping with the characteristic peak of the MWCNT [32].**

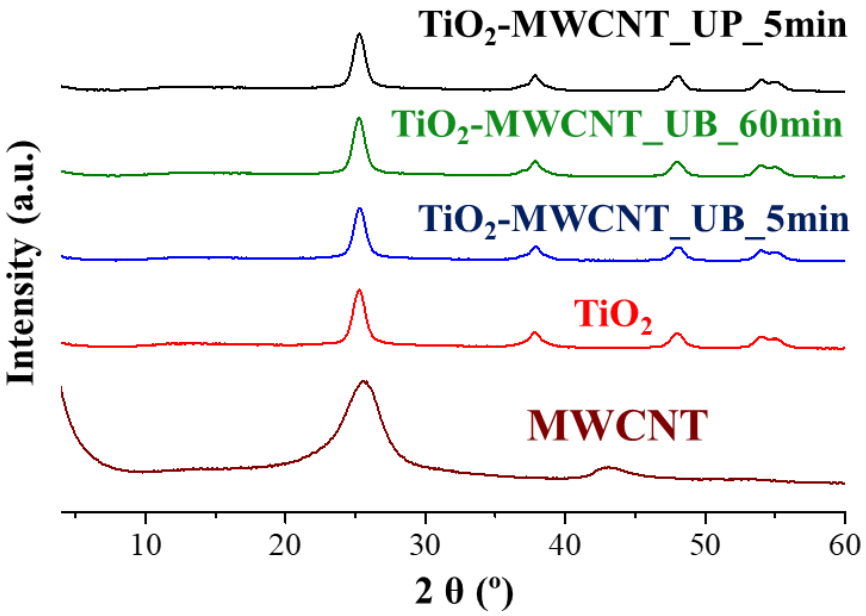

Figure 1. XRD patterns of all composites prepared with MWCNT, bare TiO_2 and pure **MWCNT** for comparison.

The UV-Vis absorption properties of the composites and the original TiO_2 were evaluated (Figure 2). The bare TiO_2 presents a band gap of 3.12 eV typical of anatase TiO_2 [31]. However, the composites presented a marked increase in the absorption of visible light and a decrease in the value of the band gap **of 3.18 eV for pure TiO_2 to 2.90 eV for the composites**, as showed in Figure 2, since MWCNTs can modify the band gap and the UV-Vis absorption properties of the semiconductor [17,33].

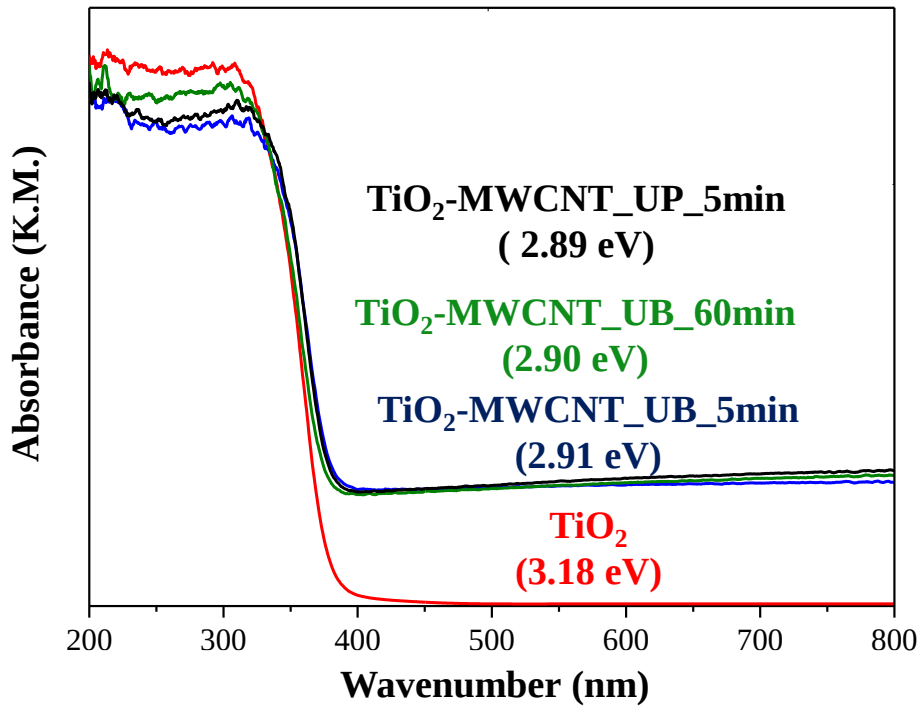

Figure 2. UV-Vis absorption spectra of the composites (TiO_2-MWCNT) and pure TiO_2.

Figure 3 presents TEM images of the composites, which show that the sample prepared after 60 minutes of sonication in a bath presents a better dispersion (smaller aggregates) than the same sample after only 5 min of sonication. Moreover in the TEM images it is observed that the sample treated using an ultrasound probe for 5 min (TiO_2-MWCNT_UP_5min) has a higher dispersion (smaller aggregates) and shorter MWCNT length with respect to the samples dispersed with an ultrasound bath (TiO_2-MWCNT_UB_5min, TiO_2-MWCNT_UB_60min), indicating that using a more powerful sonication source promotes a better dispersion of the MWCNT and may generate some structural defects in the carbon materials.

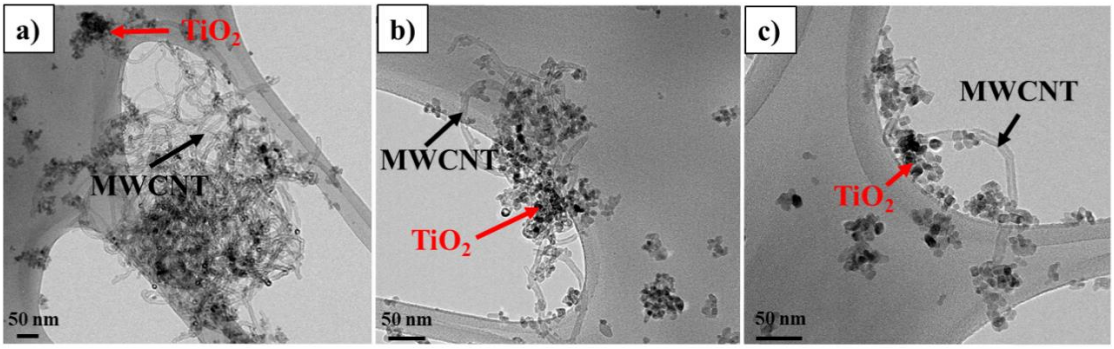

Figure 3. TEM images of the different TiO_2-MWCNT composites prepared in this work: a) TiO_2-MWCNT_UB_5min, b) TiO_2-MWCNT_UB_60min, c) TiO_2-MWCNT_UP_5min.

The interaction of the TiO_2 and the MWCNT was studied by XPS analysis (Figure 4). The XPS spectrum of Ti 2p shows a positive displacement of 0.9 eV (both Ti 2p1/2 and Ti 2p3/2 are displaced to more positive values) in presence of the MWCNT with respect to the pure TiO_2. This displacement is indicative of a good interaction between the MWCNT and the TiO_2 in the composites [34].

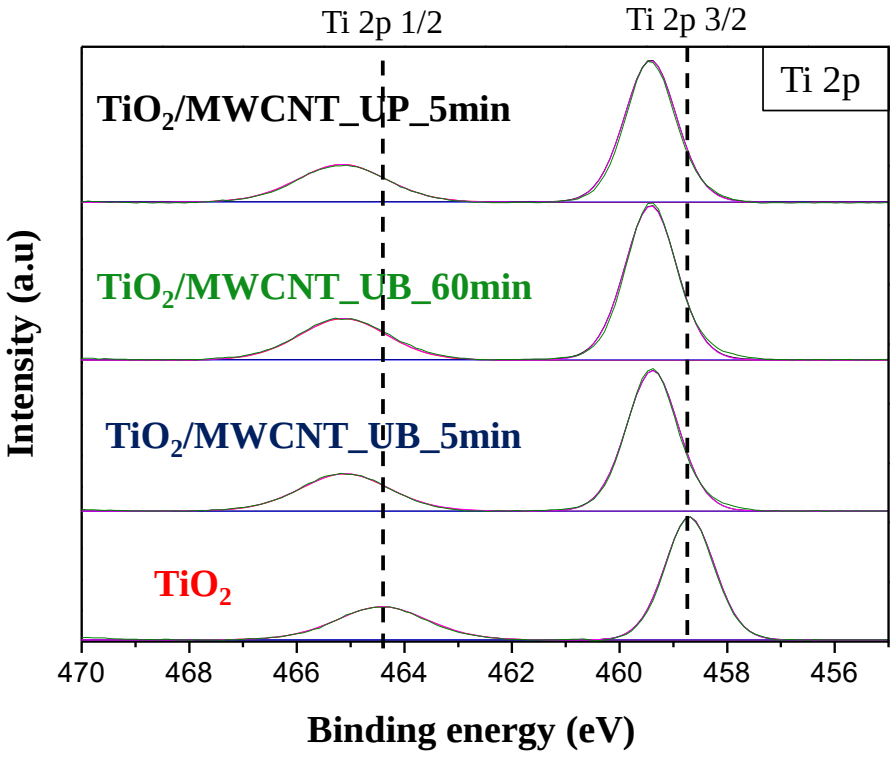

Figure 4. Ti 2p XPS spectra of the TiO_2-MWCNT composites and bare TiO_2.

In order to characterize the surface chemistry of the MWCNT after the different sonication treatments, we have determined the active surface area (ASA) and surface chemistry composition (**using** TPD) of the bare MWCNT and the MWCNT after the three different dispersion approaches. The active surface area presented in Table 2 shows an increase of ASA when the MWCNTs were sonicated for longer times (MWCNT_UB_60min) or when this carbon material was sonicated with an Ultrasonic probe (MWCNT_UP_5min). Moreover, the results obtained by TPD analysis (Table 2) showed an increase of surface oxygen groups in the MWCNT sonicated with an ultrasonic probe (MWCNT_UP_5min) with respect to the MWCNT_UB_60min, MWCNT_UB_5min and pure MWCNT samples. These parameters (ASA and surface oxygen groups) and the TEM images show that the increase of the sonication time and the use of an ultrasound probe promote a better dispersion of the MWCNT and generates some structural defects in the carbon material.

Concerning the surface oxygen groups generated in the MWCNT after the sonication process, these groups have been characterized from TPD analysis [28,29]. In this sense, the decomposition of carboxylic acids into CO_2 occurs at low temperatures and lactones decompose as CO_2 at high temperatures. Carboxylic anhydrides yield both CO and CO_2 and finally phenols, ethers, carbonyls/quinones and pyrones decompose to CO as temperature increases [28,29]. CO-TPD profiles (Figure 5 a) show a change in the surface chemistry of the CNT after sonication. Thus, samples MWCNT_UB_5min and MWCNT_UB_60min present smaller CO desorption at high temperatures and an increased desorption at lower temperatures. Moreover, sample MWCNT_UP_5min presents higher CO desorption compared to the pristine MWCNT and the sonicated with the bath, indicating an increase in the

amount of surface groups in the sample MWCNT_UP_5min (see Table 2, that includes the quantification of the evolved CO). CO_2-TPD profiles (Figure 5 a) also show interesting changes in the surface chemistry of the CNT when the samples are sonicated. In all cases, a peak appears at 300-500 ºC which is not present in the pristine CNT sample. This peak may be characteristic of carboxylic anhydrides that decompose as CO and CO_2. These results in combination of ASA analysis show that the sonication of CNT generates some structural defects in the carbon materials that may act as anchoring points, resulting in a better contact between the TiO_2 and MWCNT.

Table 2. Active surface area (ASA) and surface composition, obtained by TPD, of the pure MWCNT and only MWCNT using three different approaches used in the synthesis of the composites.

Samples	ASA (m^2/g)	CO (μmol/g)	CO_2 (μmol/g)	Total O[a] (μmol/g)
MWCNT	8.1	351	95	541
MWCNT_UB_5min	8.5	316	182	679
MWCNT_UB_60min	9.0	415	159	734
MWCNT_UP_5min	13.0	529	149	823

[a] Total O: total oxygen, calculated as $CO+2 \cdot CO_2$

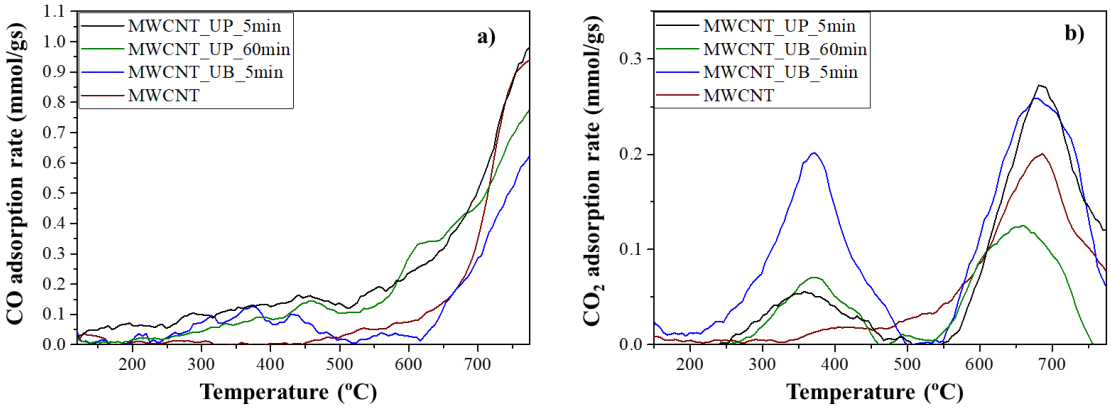

Figure 5. a) CO and b) CO_2 TPD profiles of samples MWCNT_UB_5min, MWCNT_UB_60min, MWCNT_UP_5min, and MWCNT for comparison purposes.

3.3 Photocatalytic Activity

Concerning the photocatalytic activity, we have measured the activity of the materials for the total photooxidation of propene in the gas phase at low concentration (100 ppmv in air) at room temperature. Pure TiO_2 calcined at lower temperature (350 °C) has a high propene conversion (around 60%) which surpasses the propene conversion observed for the P25 (reference sample), as showed in Figure 5. One interesting result is that the composites (TiO_2-MWCNT) synthesized in all approaches show higher conversions with respect to pure TiO_2. Moreover, we observed an increase in propene conversion for the samples prepared using an ultrasound bath for 5 min, 60 min and ultrasonic probe for 5 min, in this order: TiO_2-MWCNT_UB_5min < TiO_2-MWCNT_UB_60min < TiO_2-MWCNT_UP_5min (Figure 6). It must be noted that for the sample prepared by ultrasonic probe, an increase in activity of about 30% in propene conversion is obtained, what is quite an important improvement achieved just by adding 1wt% MWCNT. This fact can indicate that a better dispersion of the carbon materials and the generation of higher active surface area or oxygen species on the MWCNT can improve the photocatalytic activity of the composites, because it will allow a better interaction of the Ti species and the MWCNT during the sol-gel synthesis of the composites [15,17,20], thus allowing the formation of a higher amount of nuclei for TiO_2 particles growth with an effective interaction with the MWCNT as shown in Scheme 1.

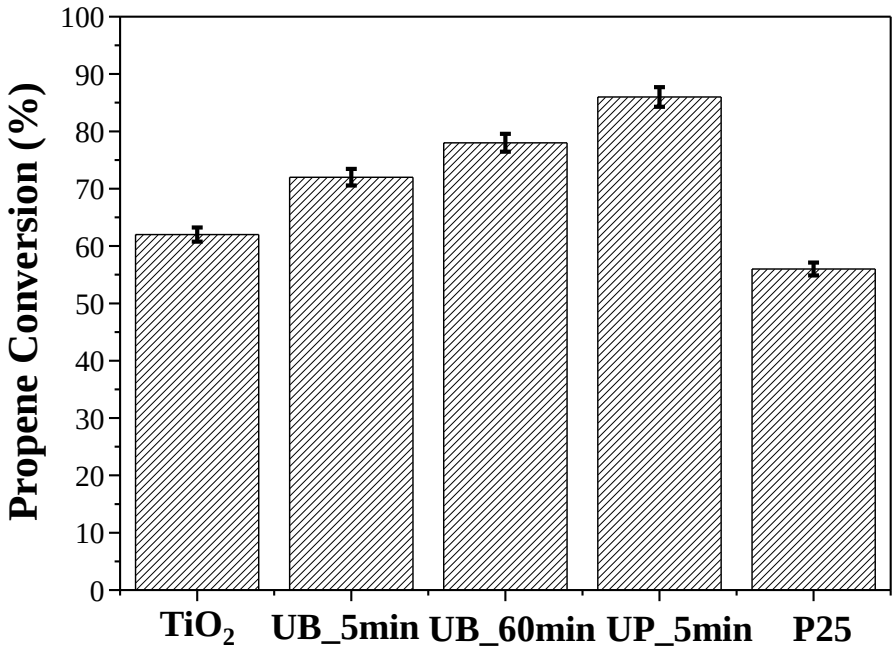

Figure 6. Propene conversion of the composites prepared in this study (TiO_2-MWCNT_UB_5min, TiO_2-MWCNT_UB_60min, TiO_2-MWCNT_UP_5min,), pure TiO_2 and commercial P25 for comparison purposes.

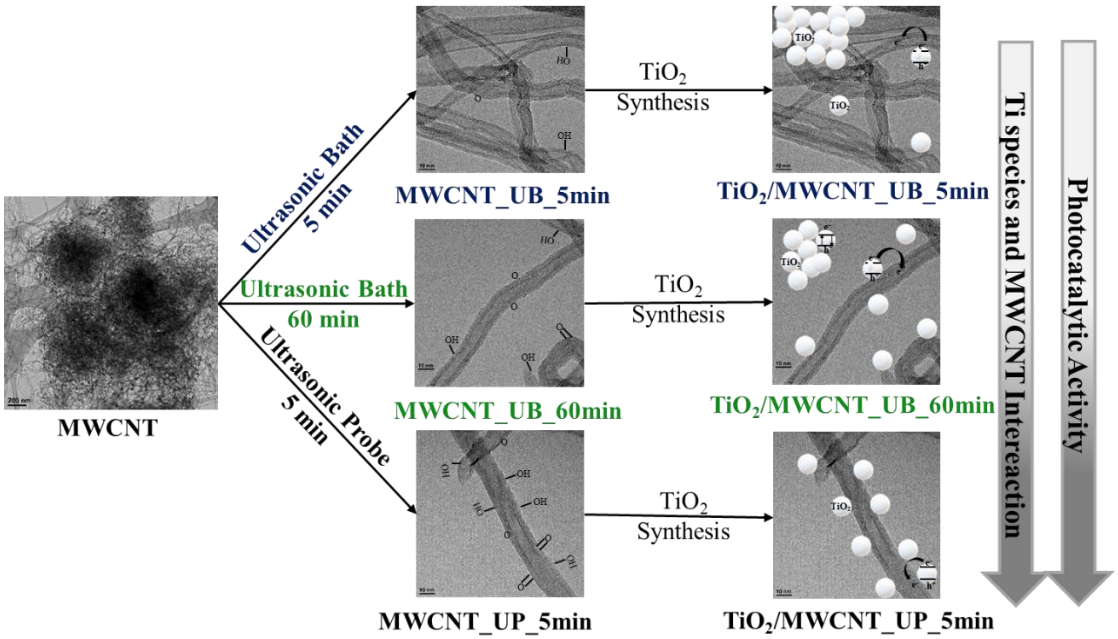

Scheme 1. Schematic representation of the synthesis procedure followed for the preparation of MWCNT-TiO_2 and the interesting results obtained in this study.

4. Conclusions

In this study, we have studied the synthesis of TiO_2-MWCNT composites focusing on the study of the effect of the dispersion of the components and of the carbon active sites of the MWCNT, on the photocatalytic properties of the composites for the abatement of propene. The most relevant results obtained were that sonicating for longer times or using a more powerful ultrasound source generates higher active surface area and surface oxygen groups on the carbon materials, which are the determining factors for the improved photocatalytic activity with respect to the bare TiO_2. These sites can act as nucleation points for Ti species during the sol-gel process that result in an efficient interaction of the TiO_2 phase with the MWCNT. This methodology can be considered as a facile approach for the synthesis of highly efficient photocatalysts based on TiO_2.

Acknowledgements

The authors thank Ministerio de Ciencia Innovación y Universidades and FEDER (Project RTI2018-095291-B-I00) and the Generalitat Valenciana (PROMETEOII/2018/076) for financial support. JFC thanks MINECO for a researcher formation grant (BES-2016-078079).

References

[1] J. Winkler, Titanium dioxide: Production, properties and effective usage, 2nd ed., Vincentz Network, Germany, 2013.

[2] K. Nakata, A. Fujishima, J. Photochem. Photobiol. C 13 (2012) 169-189.

[3] J. Schneider, M. Matsuoka, M. Takeuchi, J. Zhang, Y. Horiuchi, M. Anpo, D.W. Bahnemann, Chem. Rev. 114 (2014) 9919-9986.

[4] H. Abdullah, M.R. Khan, H.R. Ong, Z. Yaako, J. CO_2 Util. 22 (2017) 15-32.

[5] G. Liu, J.C. Yu, G.Q. Lu, H. M. Cheng , Chem. Commun. 47 (2011) 6763-6783.

[6] X. Chen, S.S. Mao, Chem. Rev. 107 (2007) 2891-2959.

[7] H. Park, Y. Park, W. Kim, W. Choi, J. Photochem. Photobiol. C 15 (2013) 1-20.

[8] S. A. Jitan, G. Palmisano, C. Garlisi, Catalyst. 10 (2020) 227.

[9] Y. Paz, Solid State Phenom. 162 (2010) 135-162.

[10] G. Jiang, X. Zheng, Y. Wang, T. Li, X. Sun, Powder Technol. 212 (2011) 284-288.

[11] R. Leary, A. Westwood, Carbon. 49 (2011) 741-772.

[12] M. Ouzzine, M. A. Lillo-Ródenas, A. Linares-Solano, Appl. Catal. B Environ. 127 (2012) 291-299.

[13] A.M. Kamil, H.T. Mohammed, A.A. Balakit, F.H. Hussein, D.W. Bahnemann, G.A. El-Hiti, Arab. J. Sci. Eng. 43 (2018) 199-210.

[14] K. Woan, G. Pyrgiotakis, W. Sigmund, Adv. Mater. 21 (2009) 2233-2239.

[15] Z. Li, L. He, L. Jing, J. Lin, Y. Luan, Chempluschem. 78 (2013) 670-676.

[16] P. Vincent, A. Brioude, C. Journet, S. Rabaste, S.T. Purcell, J. Le Brusq, J.C. Plenet, J. Non. Cryst. Solids. 311 (2002) 130-137.

[17] Y. Yu, J.C. Yu, J.G. Yu, Y.C. Kwok, Y.K. Che, J.C. Zhao, L. Ding, W.K. Ge, P.K. Wong, Appl. Catal. A Gen. 289 (2005) 186-196.

[18] W. Wang, P. Serp, P. Kalck, C.G. Silva, J.L. Faria, Mater. Res. Bull. 43 (2008) 958-967.

[19] V.B. Koli, A.G. Dhodamani, S.D. Delekar, S.H. Pawar, J. Photochem. Photobiol. A Chem. 333 (2017) 40-48.

[20] G. Jiang, X. Zheng, Y. Wang, T. Li, X. Sun, Powder Technol. 207 (2011) 465-469.

[21] G. Barrefors, G. Petersson, J. Chromatogr. A. 643 (1993) 71-76.

[22] M.S. Kamal, S.A. Razzak, M.M. Hossain, Atmos. Environ. 140 (2016) 117-134.

[23] C.F. Murphy, D.T. Allen, Atmos. Environ. 39 (2005) 3785-3798.

[24] J. Fernández-Catalá, L. Cano-Casanova, M.Á. Lillo-Ródenas, Á. Berenguer-Murcia, D. Cazorla-Amorós, Molecules. 22 (2017) 2243.

[25] B. Oregan, M. Gratzel, Nature 353 (1991) 737-740.

[26] A. Gabe, R. Ruiz-Rosas, E. Morallón, D. Cazorla-Amorós, Carbon. 148 (2019) 430-440.

[27] P.J. Hart, F.J. Vastola, P.L. Walker, Carbon, 5, (1967) 363-371

[28] M. C. Román D. Cazorla-Amorós, A. Linares-Solano, C. Salinas-Martínez de Lecea, Carbon 31 (1993) 895-902.

[29] J.L. Figueiredo, M.F.R. Pereira, M.M.A. Freitas, J.J.M. Órfão, Carbon. 37 (1999) 1379-1389.

[30] M.A. Lillo-Ródenas, N. Bouazza, A. Berenguer-Murcia, J.J. Linares-Salinas, P. Soto, A. Linares-Solano, Appl. Catal. B Environ. 71 (2007) 298-309.

[31] V.N. Kuznetsov, N. Serpone, J. Phys. Chem. B. 110 (2006) 25203-25209.

[32] Lee, D.Y., Lee, M.H., Kim, K.J., Heo, S., Kim, B.Y., Lee, S.J.: Surf. Coat. Technol. 200, 1920–1925 (2005)

[33] S. Da Dalt, A.K. Alves, F.A. Berutti, C.P. Bergmann, Part. Sci. Technol. 33 (2015) 308-313.

[34] L.A.A. Rodriguez, D.N. Travessa, Adv. Mater. Sci. Eng. 2018 (2018) 781.